

Electronic Supplementary Information (ESI)

Ethanol-Assisted Synthesis of Two-dimensional Tin(II) Halide Perovskite Single Crystals for Amplified Spontaneous Emission

*Guanchu Ding^a, Xianxiong He^a, Haihua Zhang^{*a}, Hongbing Fu^{*,a,b}*

a. Institute of Molecule Plus, Collaborative Innovation Center of Chemical Science and Engineering (Tianjin), Tianjin University, Tianjin 300072, P. R. China, E-mail: zhanghaihua@tju.edu.cn, hongbing.fu@tju.edu.cn

b. Beijing Key Laboratory for Optical Materials and Photonic Devices, Department of Chemistry, Capital Normal University, Beijing 100048, P. R. China.

Experiment

Synthesis

(TEA)₂SnI₄ (n=1) single crystals

The n=1 samples were prepared through a solution-based method. First, 2.0 mmol of 2-Thiopheneethylamine (TEA) were dissolved in 1.5 mL of Hydroiodic Acid (55-57 wt.% in water), 0.5 mL of ethanol was added to the system to help dissolve. In a separate vial, SnO (1 mmol) was dissolved in 1.5 mL of Hydroiodic Acid, 0.4 mL of Hypophosphorous acid (50 wt.% in water) were added as an antioxidant for Sn(II). The two precursors were dissolved by heating under constant magnetic stirring at 90 °C for about 3 min. Then TEAI solution was added to the SnI₂ solution, resulting in the precipitation of dark-green powder. The powder soon dissolved after adding 1.5 mL of Ethanol while heated at 90 °C, here the total usage of Ethanol is 2 mL, 37% of the total volume. The vial was transferred to a 70 °C silicone oil bath and kept for 40 min before the power turned off. After cooling down, centimeter-sized single crystals were precipitated. The crystals were washed by Dichloromethane (DCM) and dried on a filter paper without further protection. The samples were stored in a glove box for further characterization.

(TEA)₂(MA)Sn₂I₇ (n=2) single crystals

The n=2 samples were prepared with a similar method to the n=1 counterpart. First, 2 mmol of 2-Thiopheneethylamine (TEA) were dissolved in 1.5 mL of Hydroiodic Acid (55-57 wt.% in water), 0.5 mL of ethanol was added to the system to help dissolve. In a separate vial, SnO (2 mmol) was dissolved in 3 mL of Hydroiodic Acid, 0.8 mL of Hypophosphorous acid (50 wt.% in water) was added. The two precursors were dissolved by heating under constant magnetic stirring at 90 °C for about 3 min. Then TEAI solution was added to the SnI₂ solution, resulting in the precipitation of dark-green powder. Additionally, 1 mmol of CH₃NH₃Cl solid was added to the system. The powder soon dissolved after adding 4.8 mL of Ethanol while heated at 90 °C, here the total usage of Ethanol is 50% of the total volume. The system was left to room temperature naturally, about 3h later black flack crystals were obtained. The

crystals were washed by Dichloromethane (DCM) and dried on a filter paper. The samples were stored in a glove box for further characterization.

Solubility test

The test was carried at room temperature by weighing continuous weight (i.e. 0.20 g, 0.21 g, 0.22 g ...) of samples and transferred them into a vial containing 5 mL of specific $V_{\text{ethanol}}/V_{\text{HI}}$ ratio solutions. Then leave the system overnight under constant stirring. We consider the last completely dissolved vial's concentration as a certain solubility. Note that due to the instability of MASnI_3 , the solubility test of $[\text{SnI}_6]^{4-}$ layer was carried out by using MAPbI_3 instead.

Characterization

X-Ray diffraction The plate-like crystal samples were laid flat in a glass substrate. X-ray diffraction patterns were characterized using a Rigaku Smartlab 9 kw X-ray powder diffractometer with the parameter Cu K α ($\lambda=1.5405 \text{ \AA}$), diffraction angle 2θ is set from 3° to 40° , scanning speed is $10^\circ/\text{min}$.

Fluorescence and SEM microscopy Fluorescence images microscopies were acquired with a Leica DMRBE fluorescence microscope (CCD) equipped with point-enhanced band point coupling. The surface and edge images of the samples were captured by a field emission scanning electron microscope (SEM) produced by Apreo S LoVac, using ordinary and vertical aluminum sample stages, and the samples were directly pasted on the conductive adhesive and captured under the condition of an accelerating voltage of 5 kV.

Mechanical exfoliation Carefully transfer a moderately sized SC sample to Scotch tape, carefully fold the tape in half then separate, repeat several times. Finally, stick the tape to the glass substrate, and carefully separate them. A sample with a reduced thickness was left on the substrate, and the sample size was kept around $20 \mu\text{m}$ confirmed by a fluorescence microscope.

Temperature dependent PL Transfer the prepared samples to a high vacuum sample chamber refrigerated by a liquid helium compressor to 20 K. A 405 nm continuous wave (CW) laser was selected as the light source, and a specific sample was selected with the help of a CCD system. The sample was excited, and the PL signal was collected using a grating spectrometer with a resolution of 0.1 nm from 20 K. The liquid helium compressor was operated to warm it up, and spectra were collected every 30 K to 290 K. Integrate the area of the collected PL spectrum to obtain its intensity (I), draw an I-(1/T) image, and fit the data.

ASE and TR-PL characterization A 400 nm, 150 fs, 1000 Hz pulsed laser (Tisapphire sapphire laser) was selected as the light source. In both tests, the light source was focused on a uniform spot with a diameter of $100 \mu\text{m}$ to excite the sample. μ -PL spectra were recorded in reflection mode, and the PL signal or time-resolved PL (TR-PL) signal

was detected by a streak camera. For the ASE test, we adjusted the pump light intensity by rotating the attenuation wheel to obtain PL spectra under different excitation light intensities and used a grating spectrometer to collect the signals. For time-resolved spectroscopic (TR-PL) characterization, we used a streak camera (C5680, Hamamatsu Photonics) equipped with a polychromator (250is, Chromex) with a temporal resolution of 10 ps. At 20 K, keep the temperature and excitation light energy unchanged, record the photon decay process of the sample in a specific wavelength range.

In our scenario, the single crystals were exfoliated into small-sized ($\sim 30 \mu\text{m}$) flakes (Fig. S8). Therefore, the Variable Stripe Length is not suitable. In our experiment, the excitation laser was focused into a uniform 100- μm -diameter spot covering the exfoliated crystal. Our crystal showed strong in-plane optical confinement and effective 2D waveguiding behavior, facilitating to achieve optical feedback for ASE. Therefore, we used a circular beam spot to confirm the occurrence of ASE. The ASE signals are collected in front of the exfoliated flakes as a function of the pump density. The size, thickness, and stability of our exfoliated crystals can affect the ASE threshold.

Supporting figures

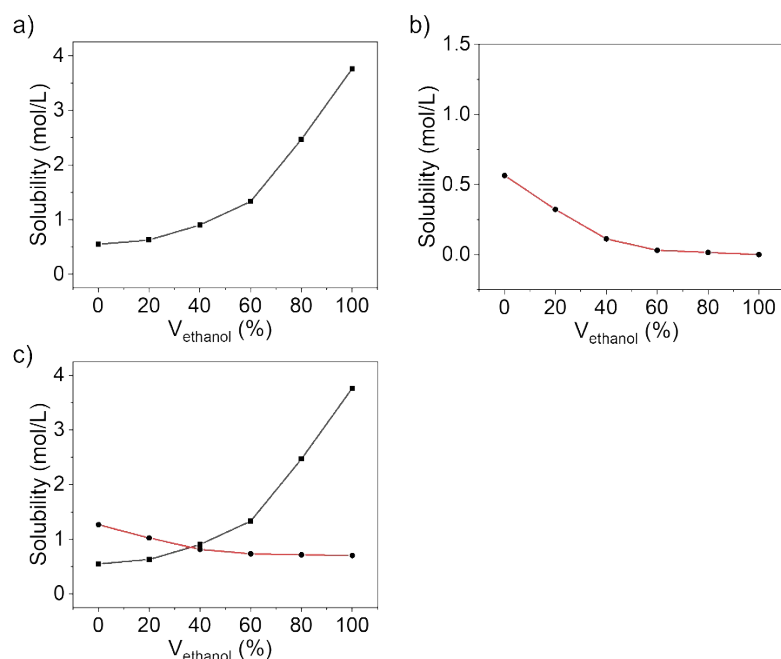


Fig. S1 Solubility curve of perovskite precursors under different ethanol volume ratios in HI aqueous solution. (a) (TEA)I and (b) (MA)PbI₃. (c) TEAI (black line) and proposed (MA)SnI₃ (red line).

It can be seen from Fig. S1a that the solubility of TEAI increased from 0.55 to 3.76 mol L⁻¹ with ethanol volume ratio increasing from 0% to 100%. Because tin(II) is easily oxidized under ambient conditions, we measured the solubility of [PbI₆]⁴⁻ (MAPbI₃) to model and deduce the solubility trend of [SnI₆]⁴⁻. It can be seen from Figure S1b that that the solubility of [PbI₆]⁴⁻ (MAPbI₃) decreases from 0.57 to 0.001 mol L⁻¹ as the ethanol volume ratio increased from 0% to 100%. Therefore, different trends of TEAI and [SnI₆]⁴⁻ solubility allow us to modulate the supersaturation and the ratio of precursors in mixed solution by changing the ethanol volume ratio. As proposed in Fig. S1c, we speculate that solubility of [SnI₆]⁴⁻ is higher than that of TEAI at the ethanol volume ratio of 0% and reach a balance point at 37%, where desired single-crystals precipitate according to the stoichiometric ratio with improved crystallinity and size.

V_{ethanol} in V_{HI} (%)	Solubility of (TEA)I (mol/L)	Solubility of (MA)PbI ₃ (mol/L)
0 (HI)	0.549	0.565
20	0.627	0.323
40	0.901	0.113
60	1.332	0.032
80	2.469	0.016
100 (ethanol)	3.763	0.001

Table S1 Solubility data of iodine 2- thiophene ethylamine (TEAI) and MAPbI₃. With the increase of ethanol volume in HI, the solubility of TEAI show an increasing trend, while the solubility of MAPbI₃ shows a slightly decreasing trend.



Fig. S2 Pre-test of TEA₂SnI₄ SCs. The vial marked means the volume ratio of ethanol versus HI. When ethanol was added up to 60 %, there were no product.

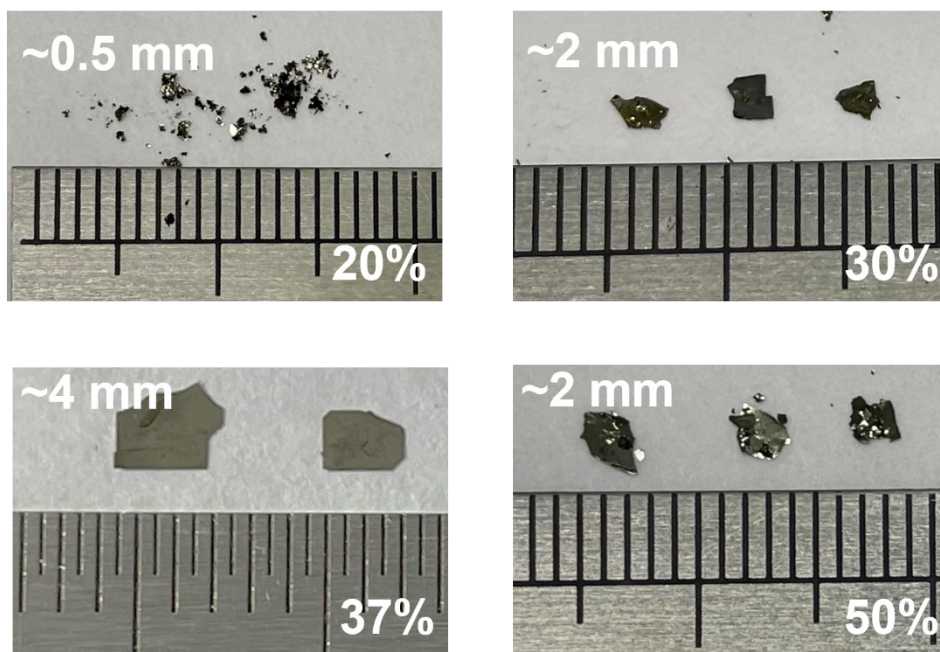


Fig. S3 We carried the whole synthesis routine with different ethanol volume ratios including the slowly cooling process when deciding the optimal ethanol ratio. Taking the ethanol volume ratio of 20%, 30% ,and 50% for example, the samples reveal smaller size (~0.5 mm for 20%, ~2 mm for 30% and ~2 mm for 50%) and worse crystallinity (as shown in the corresponding pictures) compared to the product with 37% ethanol added (~4 mm with improved crystallinity).

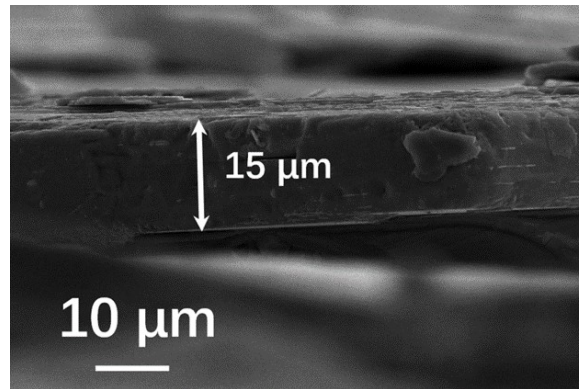


Fig. S4 SEM image of TEA₂MA₂Sn₂I₇ (n=2) single crystal's side, the thickness of prepared sample is estimated to be 15 μm, lower than that of n=1 counterparts, which is unqualified for Single Crystal X-Ray Diffraction test.

Identification code		(TEA) ₂ SnI ₄
Empirical formula		I ₄ SnC ₁₂ H ₂₀ N ₂ S ₂
Space group		$p\bar{1}$
Crystal system		triclinic
Cell length	a/Å	8.6029(3)
	b/Å	8.6074(5)
	c/Å	15.7761(9)
Cell Angles	$\alpha/^\circ$	81.216(5)
	$\beta/^\circ$	83.095(4)
	$\gamma/^\circ$	89.892(4)
Volume/Å ³		1145.96
Z		2

Table S2 Single crystal X-ray Diffraction data of TEA₂SnI₄

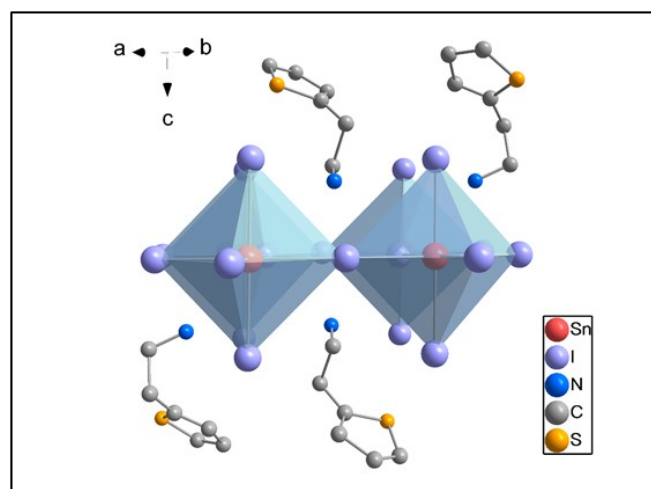


Fig. S5 Single crystal structure of TEA₂SnI₄.

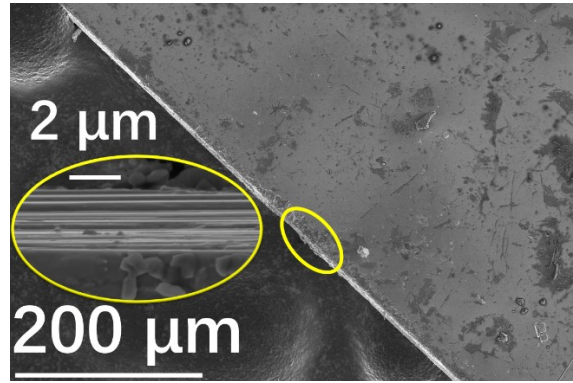


Fig. S6 SEM image of TEA₂SnI₄ crystal's surface and side

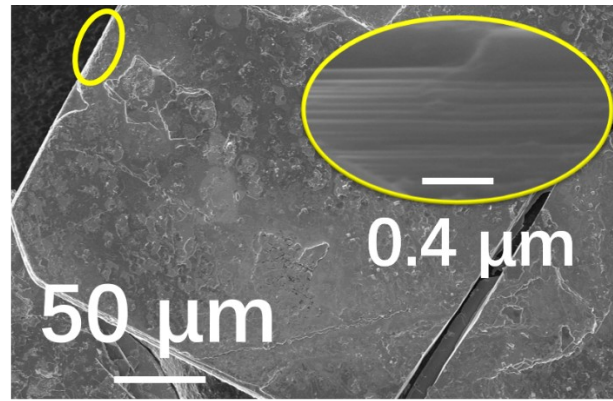


Fig. S7 SEM image of TEA₂MASn₂I₇ crystal's surface and side.

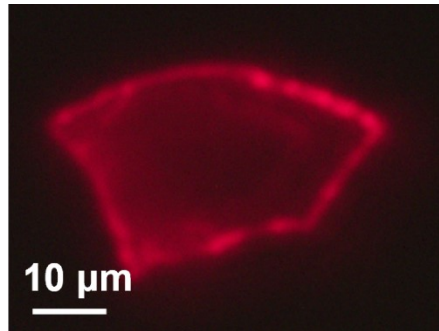


Fig. S8 The fluorescence picture of $n=1$ single crystal pumped by 400nm femtosecond laser with high pumped density at 20 K. The bright-emissive edge and weak-emissive body indicate strong in-plane optical confinement and effective 2D waveguiding behavior.

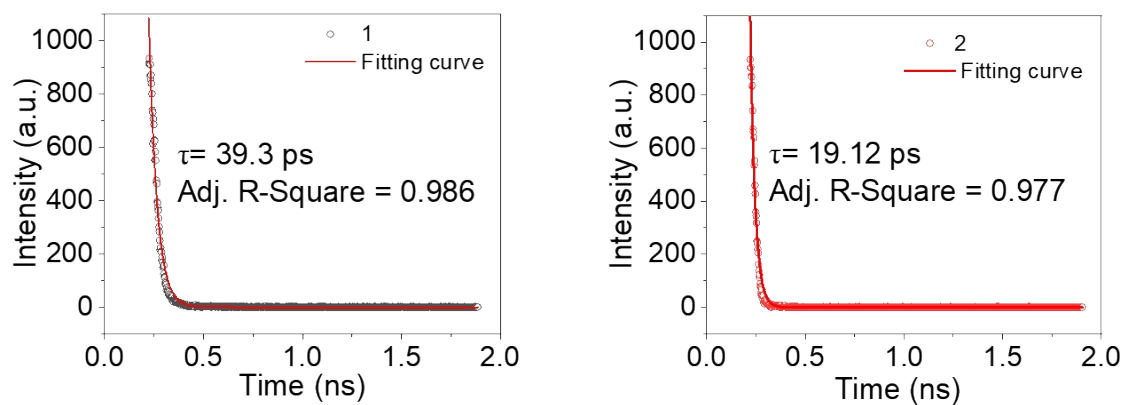


Fig. S9 Fitting results of TR-PL of TEA₂SnI₄. The lifetime of 1 and 2 (below and above the threshold) is 39.3 ps and 19.12 ps respectively.

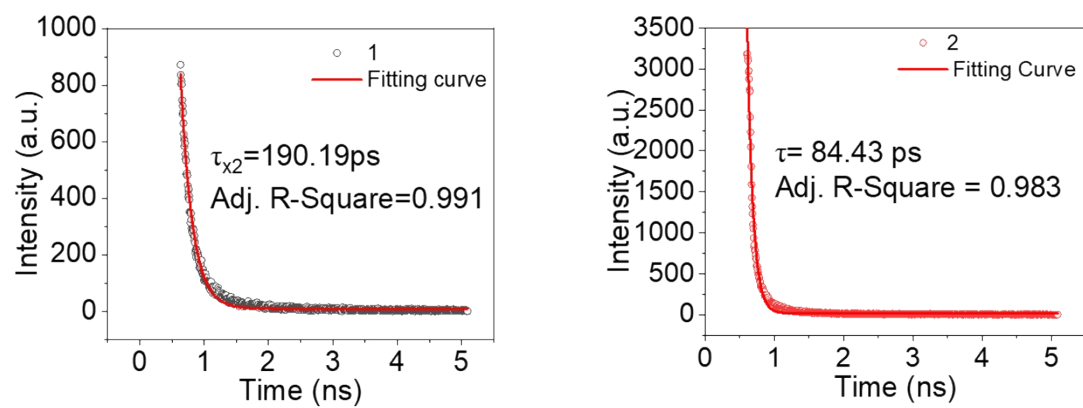


Fig. S10 Fitting results of TR-PL of TEA₂MASn₂I₇. The lifetime of 1 and 2 (below and above the threshold) is 190.19 ps and 84.43 ps respectively.

Compound	Compound Type	Temperature	λ_{ASE} or laser/nm	Threshold / $\mu\text{J cm}^{-2}$	Ref.
α -6T	Organic	10 K	589	35	1
BC4	Organic	R.T.	499	27	2
BP3T	Organic	R.T.	618	8	3
2FCz	Organic	R.T.	427	5	4
6PP	Organic	R.T.	490	12.1	5
2L-F	Organic	R.T.	430	12	6
4L-F	Organic	R.T.	457	17	6
(BA) ₂ (MA) ₂ Pb ₃ I ₁₀	2D Perovskite (exfoliated SC)	78 K	630	2.6	7
(BA) ₂ (MA) ₂ Pb ₃ I ₁₀	2D Perovskite (thin flakes)	20 K	627	5.8	8
(TEA) ₂ SnI ₄	2D Perovskite (exfoliated SC)	20 K	674	29.1	Our work
(TEA) ₂ (MA)Sn ₂ I ₇	2D Perovskite (exfoliated SC)	20 K	755	630.1	Our work

Table S3 Comparison of ASE properties of our 2D tin-based perovskite single crystals with recently reported organic gain molecules and 2D perovskite materials. Note that different from the commonly used Variable Stripe Length method, in our work, a circular spot beam was used to excite the sample, which may cause different results.

References

1. D. Fichou, S. Delysse and J.-M. Nunzi, *Adv. Mater.*, 1997, **9**, 1178–1181.
2. M. Ichikawa, R. Hibino, M. Inoue, T. Haritani, S. Hotta, T. Koyama and Y. Taniguchi, *Adv. Mater.*, 2003, **15**, 213–217.
3. M. Ichikawa, K. Nakamura, M. Inoue, H. Mishima, T. Haritani, R. Hibino, T. Koyama and Y. Taniguchi, *Appl. Phys. Lett.*, 2005, **87**, 221113.
4. M. Wei, M. Fang, S. K. Rajendran, W.-Y. Lai, G. A. Turnbull and I. D. W. Samuel, *Adv. Photonics Res.*, 2020, **2**, 2000044.
5. Y. Jiang, K. F. Li, K. Gao, H. Lin, H. L. Tam, Y. Y. Liu, Y. Shu, K. L. Wong, W. Y. Lai, K. W. Cheah and W. Huang, *Angew. Chem. Int. Ed.*, 2021, **60**, 10007-10015.
6. M. Wei, M. Fang, S. K. Rajendran, W.-Y. Lai, G. A. Turnbull and I. D. W. Samuel, *Adv. Photonics Res.*, 2020, **2**, 2000044.
7. Y. Liang, Q. Shang, Q. Wei, L. Zhao, Z. Liu, J. Shi, Y. Zhong, J. Chen, Y. Gao, M. Li, X. Liu, G. Xing and Q. Zhang, *Adv. Mater.*, 2019, **31**, e1903030.
8. X. He, H. Gong, H. Huang, Y. Li, J. Ren, Y. Li, Q. Liao, T. Gao and H. Fu, *Adv. Opt. Mater.*, 2022, 2200238.